Progress in Visualization, Volume 1, 1992

ATLAS OF VISUALIZATION

V.S.J.

Edited by The Visualization Society of Japan

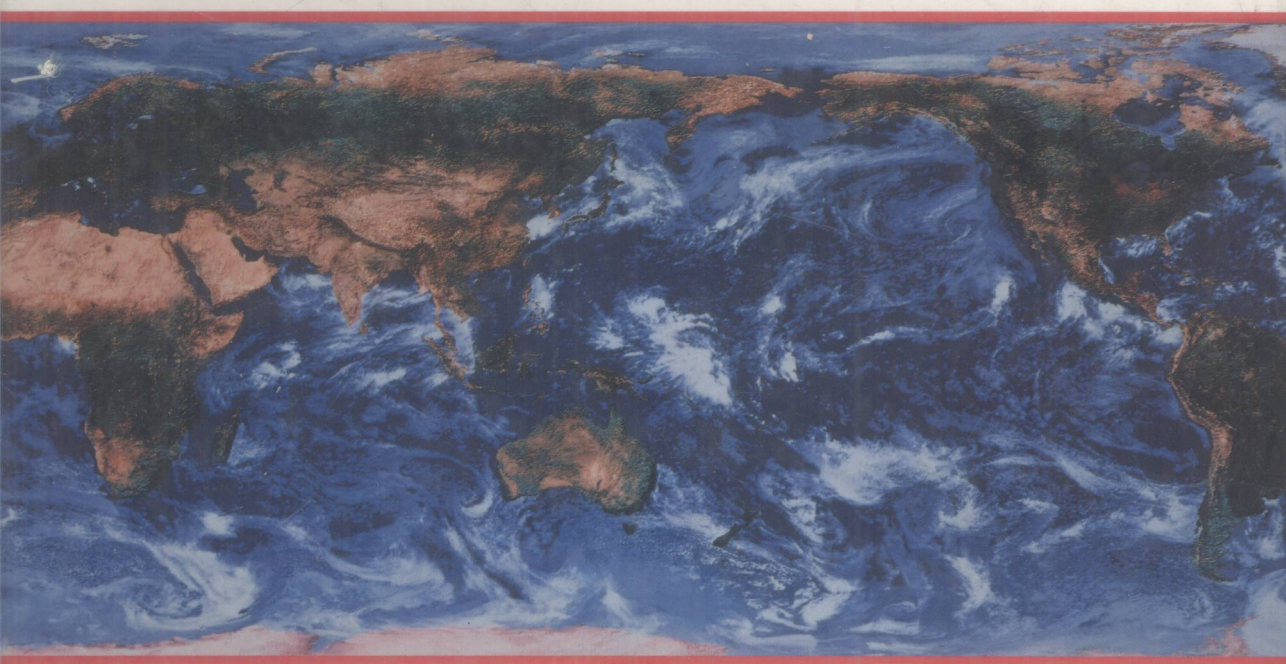

PERGAMON PRESS

ATLAS OF VISUALIZATION

Edited by

The Visualization Society of Japan

PERGAMON PRESS

OXFORD · NEW YORK · SEOUL · TOKYO

UK Pergamon Press Ltd, Headington Hill Hall, Oxford OX3 0BW, England

USA Pergamon Press Inc, 660 White Plains Road, Tarrytown, New York 10591–5153, USA

KOREA Pergamon Press Korea, KPO Box 315, Seoul 110–603, Korea

JAPAN Pergamon Press Japan, Tsunashima Building Annex, 3–20–12 Yushima, Bunkyo-ku, Tokyo 113, Japan

---

First edition 1993

British Library Cataloguing in Publication Data
A catalogue record for this book is available from the British Library.

Library of Congress Cataloguing-in-Publication Data

A catalogue record for this book is available from the Library of Congress

0 08 041909 7

Filmset by Selwood Systems, Midsomer Norton

Printed in Great Britain by Butler & Tanner Ltd, Frome and London

ATLAS OF VISUALIZATION

PROGRESS IN VISUALIZATION

Volume 1

Pergamon Titles of Related Interest

DIXON
Fluid Mechanics, Thermodynamics of Turbomachinery, 3rd Edition

DUNN & REAY
Heat Pipes, 4th Edition

HAYWOOD
Analysis of Engineering Cycles, 4th Edition

HAYWOOD
Analysis of Engineering Cycles, Worked Problems

JAPAN SOCIETY OF MECHANICAL ENGINEERS
Visualized Flow

REAY & MACMICHEAL
Heat Pumps, 2nd Edition

Pergamon Related Journals (*free specimen copies available on request*)

Building and Environment

Computers and Fluids

Computers and Graphics

Computers and Structures

Computing Systems in Engineering

International Journal of Heat and Mass Transfer

International Journal of Multiphase Flow

International Journal of Mechanical Sciences

International Journal of Solids and Structures

Structural Engineering Review

List of Editors

L. M. FINGERSON (TSI)
L. HESSELINK (Stanford University)
B. KHALIGHI (GMRL)
J. H. KIM (EPRI)
C. MARINO (Cray Research Inc.)
H. M. NAGIB (Illinois Institute of Technology)
S. ROBINSON (Langley, NASA)
V. R. WATSON (Ames, NASA)

Japan

R. KIMURA (University of Tokyo)
H. NAKAGAWA (Kyoto University)
S. MURAKAMI (University of Tokyo)
K. TAKAYAMA (Tohoku University)
T. TANAHASHI (Keio University)
K. TSUCHIYA (Waseda University)
M. YANO (Kobe University)

Advisory Board

R. J. GOLDSTEIN (University of Minnesota)
S. J. KLINE (Stanford University)
F. J. WEINBERG (Imperial College)
T. ANDO (Keio University)
T. ASANUMA (University of Tokyo)
T. HAYASHI (Chuo University)
M. HINO (Tokyo Institute of Technology)
I. IMAI (Kogakuin University)
H. OHASHI (Kogakuin University)
S. TANEDA (Kurume Institute of Technology)

Preface

Since ancient times, man has attempted to decorate vessels and bells with patterns of waves and fires. This might well have come from their worship of their God or super-power in nature. Clearly from the distant past man has observed and visualized nature with reverence.

It is well known that Leonardo da Vinci left some sketches of the vortical flow behind obstacles in the medieval age. This may be the first scientific approach to flow visualization. In the last century, natural science has made rapid progress. Indeed, an epoch-making discovery in fluid dynamics was made by O. Reynolds through a flow visualization technique (dye-tracer method) that clarified the transition from laminar to turbulent flow to be governed by a non-dimensional parameter crowned his name. Since then, flow visualization techniques have played important roles to elucidate flow phenomena, particularly to create new concepts such as the boundary layer by L. Prandtl (particle-suspension method) and the bursting mechanism in the generation of turbulence by S. Kline (H_2-bubble method).

It is also noted that the optical method has considerably advanced the field of high-speed aerodynamics and brought about today's prosperity of aircraft. The invention of Laser has led to a revolutional progress in visualization by the optical method, creating new methods such as holography and the speckle method. Lasers are now widely used in flow visualization as light sources and also as signal carriers in laser optical systems.

Flow visualization is originally used to gain information of the whole flow field observed. This improves the ability to grasp the physical characteristics of phenomena qualitatively but leads to the difficulty in quantitative analysis of flow.

Over the last decade, advances in computer technologies have brought great changes to the field of flow visualization. Particularly in the form of image processing and computer graphics, namely computer-aided flow visualization (CAFV). These technologies are now being used to great effect for quantitative analysis in flow visualization, a capability which this field had previously lacked. They have also made it possible to visualize nonvisual information in living bodies, termed computer tomography (CT). Numerical calculation has also come to be recognised as a partner of flow visualization with regard to computational fluid dynamics (CFD). Even now we are seeing flow visualization expand to cover a range of information generally thought of as nonvisual, such as heat and mass transfer, acoustic energy flow, electromagnetic flow etc.

To reflect these advances, the Visualization Society of Japan was established

in 1990, succeeding the Flow Visualization Society of Japan. The scope are now far broader than that of its predecessor, covering much wider special fields and reflecting the inclusion of computer-aided methodologies. The VSJ is responsible for many projects aimed at disseminating and promoting exchange of information. Publications include the journal *Kashika-Joho* (Visualization Science & Technology), the Handbook of Flow Visualization, and a compilation of photographs of flow visualization. All these publications have proved popular, and there are now being published a journal of English-language editions. This new series will be published annually at first with the intention to increase the frequency of publication as the series expands. *Progress in Visualization* will not only be concerned with the fields of engineering and physics but also with other fields such as medical science, agriculture, marine products, oceanography, meteorology and sports. Its aim is to provide a medium for announcing advances in visualization techniques, image processing, visualization of measured and computed results, and computer graphics to readers in many disciplines. *Progress in Visualization* will be issued in full color, so that the complex phenomena may be presented clearly and combined phenomena may be illustrated in quantitative results and detailed structure.

The VSJ has been responsible for organizing national and international symposia, seminars, workshops, conferences, etc. The results of these meetings will also be reflected in *Progress in Visualization*. The VSJ is open to people from all countries, and participation in its international activities is welcome.

Finally, on behalf of the Editorial Board, I would give my sincere acknowledgement to the authors who presented their worthy papers and photographs to this first issue, and hope that much more interdisciplinary and worldwide cooperation will be promoted through this series.

Y. TANIDA
Editor-in-Chief

Frontispiece Illustrations

FIGURE 1.	S. J. Kline	*Stanford University, USA*
FIGURE 2.	J. M. Desse	*ONERA, France*
FIGURE 3.	J. M. Desse	*ONERA, France*
FIGURE 4.	C. J. Chen	*Florida State University, USA*
FIGURE 5.	R. J. Adrian	*University of Illinois, USA*
FIGURE 6.	H. M. Nagib	*Illinois Institute of Technology, USA*
FIGURE 7.	L. C. Chen	*University of Iowa, USA*
FIGURE 8.	L. C. Chen	*University of Iowa, USA*
FIGURE 9.	M. Coutanceau	*University of Poitiers, France*
FIGURE 10.	T. Sakata	*Tokai University, Japan*
FIGURE 11.	T. Kumagai	*National Research Institute for Earth Science and Disaster Prevention, Japan*

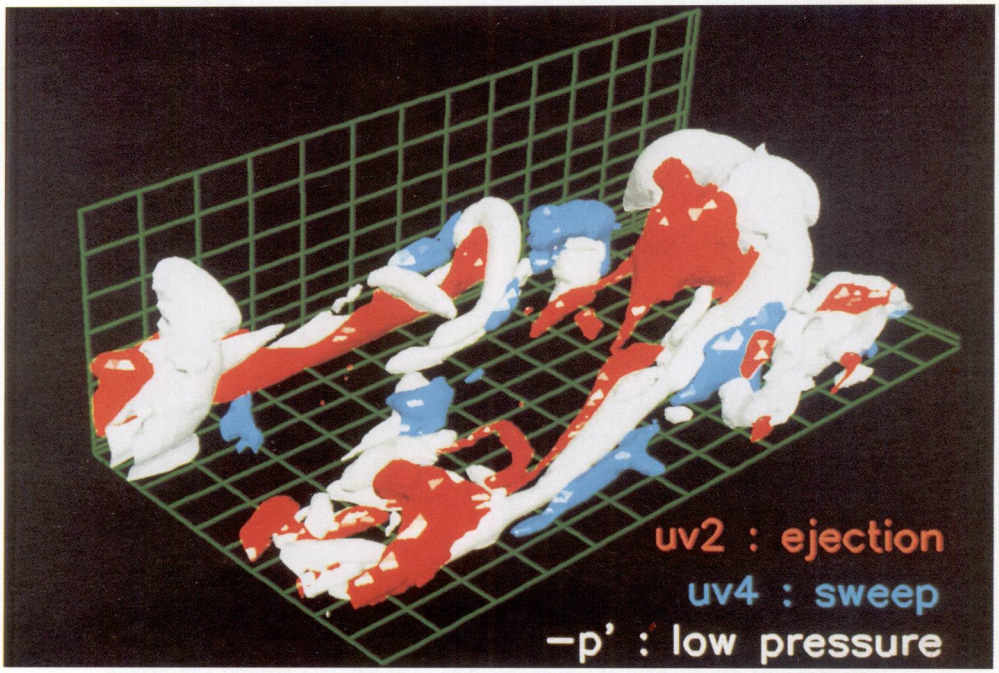

FIG. 1. Quasi-coherent structures in the turbulent boundary layer.

The picture shows a top view of a volume taken from Pilippe Spalart's database for the flat at $R = 670$. The volume is 845 wall units in the x (flow) direction and 418 wall units in the z direction (cross stream along the plate). The white contour surface shows low pressures at a value of $p'/(u_\tau)^2 = -4.2$, and indicates vortices. The red contour surface indicates an ejection motion as shown by a value of $uv2/(u_\tau)^2 = -4.2$ (second quadrant Re stress). The blue surface indicates a sweep as shown by a value of $uv4/(u_\tau)^2 = -4.2$ (fourth quadrant Re stress). Notice that second quadrant Re stress occurs in two places: (1) underneath and behind the transverse vortex head; (2) inboard (head side) of the tilted streamwise vortex leg near the wall. The $uv4$ also occurs in two places: (1) outboard of the leg vortex; (2) outboard of the neck portion of the vortex. These spatio-temporal relations are the common pattern, although other patterns do occur.

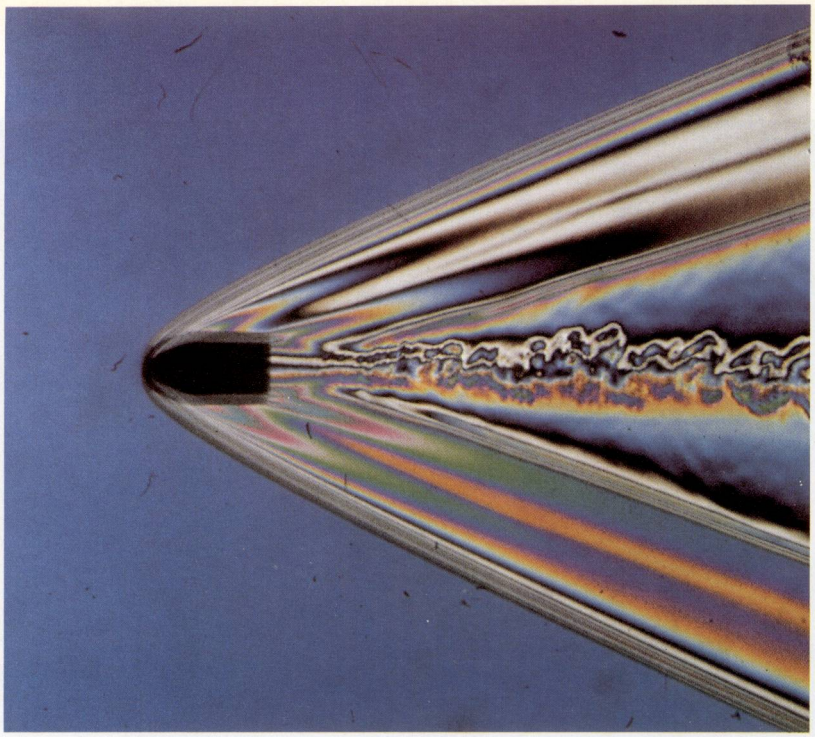

FIG. 2. Flow around a projectile.

Instantaneous density field of supersonic flow of Mach 2.77 around a projectile is shown. The optical set-up, Strio-interferometer SD200, developed at the IMFL uses a Wallaston prism differential interferometer, white flashlight and high-speed rotating prism camera, CORDIN 350, producing up to 35,000 frames per second at its maximum speed.

Shock waves and wake flow behind the projectile are clearly captured with horizontal fringes under the condition of uniform background colour and a very large birefringence angle.

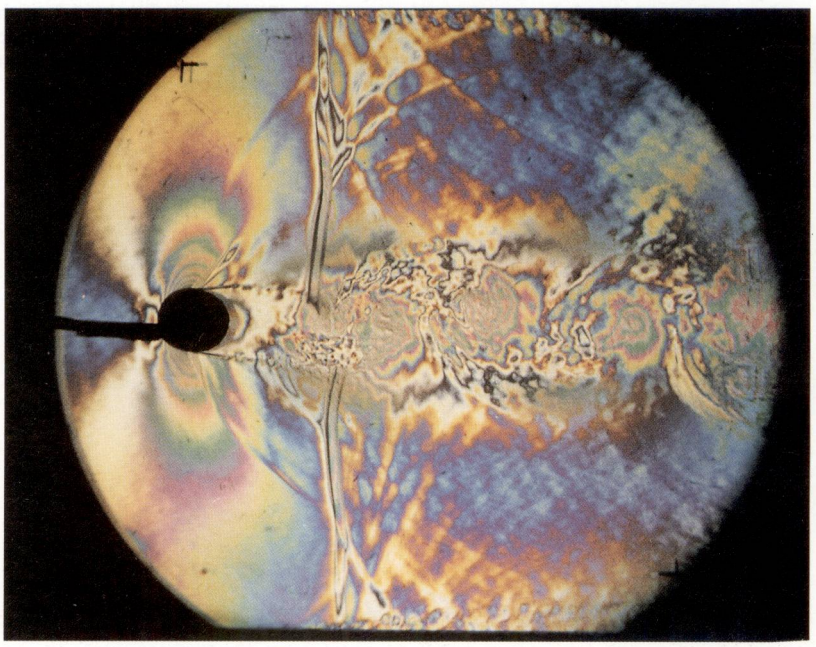

FIG. 3. Flow around a circular cylinder. Instantaneous density field of flow around a circular cylinder is shown. Inflow from left to right approaches the cylinder at Mach 0.8. The optical set-up introduced in the test is the same as described in Fig. 2.

Wake flow, downstream vortices, and accerelating flow vicinity of the cylinder and these complex mixings are clearly observed with vertical fringes.

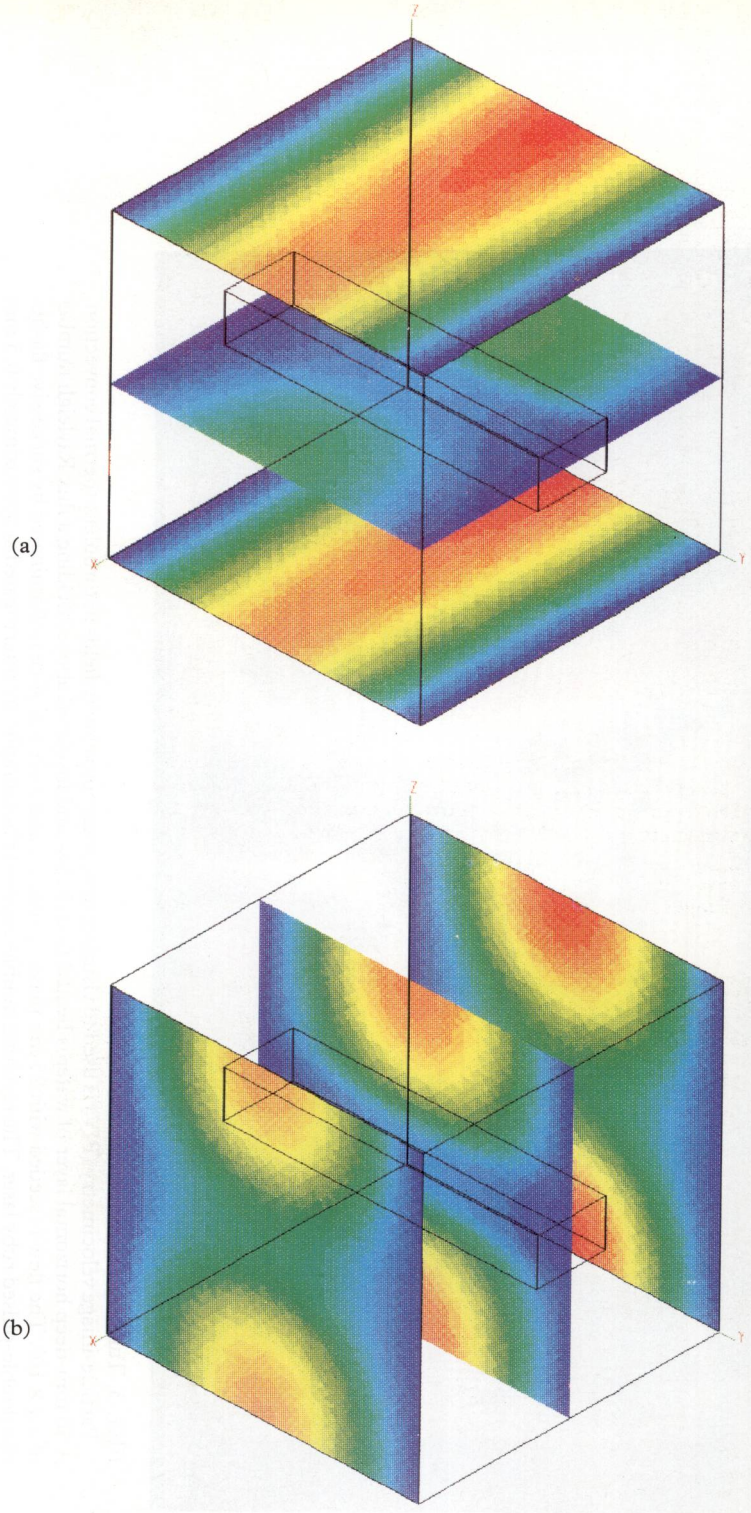

FIG. 4 (a) AND (b). Convection heat transfer in a finned passage of a compact heat exchanger.

These pictures display the velocity and temperature distribution inside two parallel plates in a compact heat exchanger. These plates are connected by an array of heat conducting fins. These results were obtained using the finite analytic numerical method in a representative three-dimensional subdomain of the heat exchanger. In this subdomain, a hot fluid flows between the two cold plates connected by a heat conducting fin. Figures 4 (a) and (b) render the temperature distribution on three cross-sections parallel and perpendicular to the flow respectively.

FIG. 5. Turbulent thermal convection.

Particle-image velocimetry (PIV) is used to visualize instantaneous velocity fields in turbulent thermal convection. A 50 mm-deep horizontal layer of water is heated from below and insulated above, yielding a flux Rayleigh number of 1.1×10^8. The flow is seeded with 25 μm plastic particles, and a vertical slice is illuminated by successive flashes of a double-pulsed ruby laser. The resulting double-exposed photographs are interrogated at approximately 0.5 mm horizontal and vertical intervals, giving in-plane velocity components at 20,800 points. Numerical differentiation of the velocity fields provided instantaneous fields of vorticity, shown in the figure, visualized by colour-coding according to the scale to the right of the figure. The velocity vectors are overlayed.

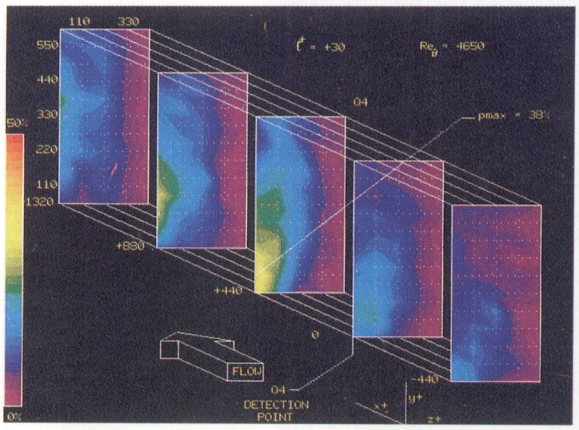

FIG. 6. Three-dimensional representation of turbulence producing events in a boundary layer.

The events which are responsible for the majority of the turbulence production in the near-wall region of a turbulent boundary layer have been investigated at a Reynolds number based on momentum thickness of 4650. Using multiple cross-wires, the streamwise (u) and normal (v) velocity components were measured in a three-dimensional grid simultaneously with u and v at a detection point located at $y^+ = 35$. Conditional space–time probability density distributions were calculated at all measurement locations based on the occurrence of a turbulence-producing event at the point of detection. the colour at each grid point represents the probability of observing a sweep (Q4) event at the grid point simultaneously with a sweep (Q4) event at the detection point. The resulting representation of the 3-D flowfield demonstrates that a significant fraction of the turbulence-producing events are relatively large in scale, and that a hierarchy of sizes exists.

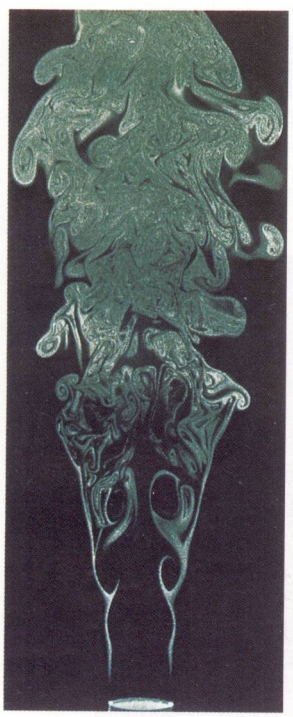

FIG. 7 (LEFT). A reactive Mie scattering visualization of the nearfield of cold jets.

The experiments were conducted in a vertical, coaxial jet facility. The central jet was surrounded by a low-velocity (0.16 m/s) air flow to shield the jet from outside disturbances. The jet nozzle has a sharp contraction, yielding an inside diameter of 10 mm from a 25-mm tube.

$TiCl_4$ vapour was seeded to the dry jet fluid. $TiCl_4$ vapour reacts with the H_20 vapour in air to form micron-sized $Ti0_2$ particles. A laser-light sheet was used for visualization. The light source was a frequency doubled, pulsed (-10 ns) Nd:YAG laser.

Roll-up vortices were observed in the initial shear layer of the jet. These vortices merged near the end of the potential core; three-dimensional vortices were formed.

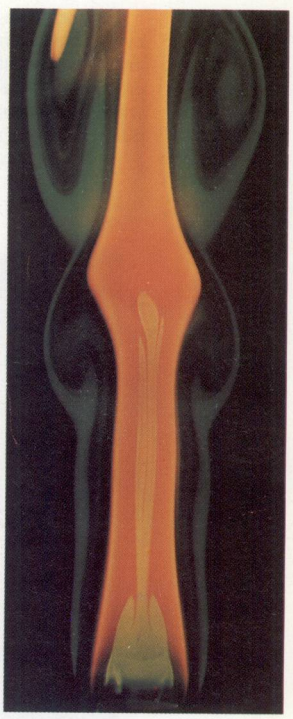

FIG. 8 (RIGHT). A reactive Mie scattering visualization of low-Reynolds number propane diffusion flames.

The experiments were conducted in a vertical combustion tunnel. The fuel jet (22 mm tube) was surrounded by a low-velocity (0.16 m/s) air flow to shield the jet from outside disturbances. The same visualization apparatus and technique as Fig. 7 were used for this phenomena.

TiO_2 particles (green colour) marked the convective mixing between the fuel jet and combustion products inside the luminous flame (orange colour) and that between the surrounding air and combustion products outside the luminous flame. Large toroidal vortices outside the luminous flame and a shedding recirculation zone above the burner tube, inside the flame, are observed.

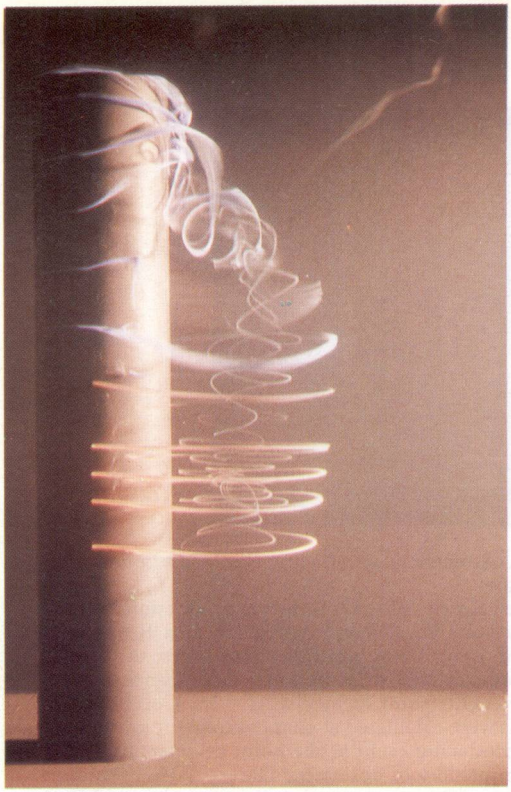

(a)

FIG. 9 (a) AND (b). Flow induced by a short circular cylinder.

A short circular cylinder with aspect ratio of 5 (the diameter is 5 cm) is impulsively set into translation from rest in a vertical water tank. Note that pictures are tilted 90 degrees so that water flows from left to right. One end of this cylinder is free, the other end is fixed to a flat plate. The Reynolds number, based on the cylinder diameter, is 1000.

The flow visualization is realized with a dye technique. The dye (Silicon oil "Rhodorsil" with printing ink) is emitted from the cylinder surface by small holes ($\varnothing = 0.6$ mm). It is illuminated by a projecter of 300 w. The photographs show the results at the time of $t^* = 3.5$. where the time unit ($t^* = 1$) corresponds to a translation of the cylinder of one diameter.

Figure 9 (a) presents the 3-D structure of the flow. In particular, it clearly evidences spanwise propagation of the perturbation induced both by the free end and the flat plate. Furthermore, it shows a starting vortex pair formed at the free end and convected by the main flow. On the other hand, Fig 9 (b) shows the near wake development (primary and secondary vortices) and the loss of symmetry which occurs before the shedding vortex process. In this case, only the dye holes located near the end plate support ($1.0 \leq 1/D \leq 2.5$) were open.

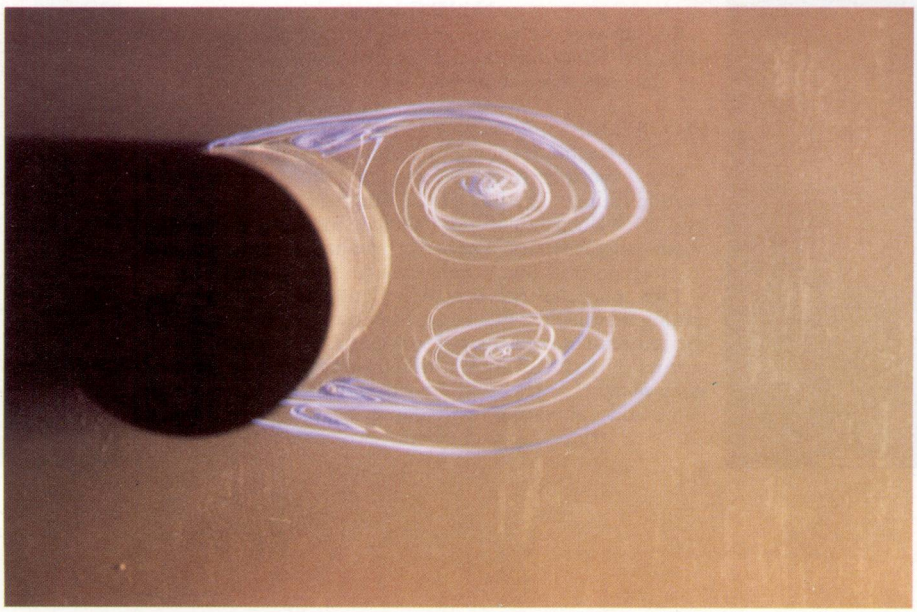

(b)

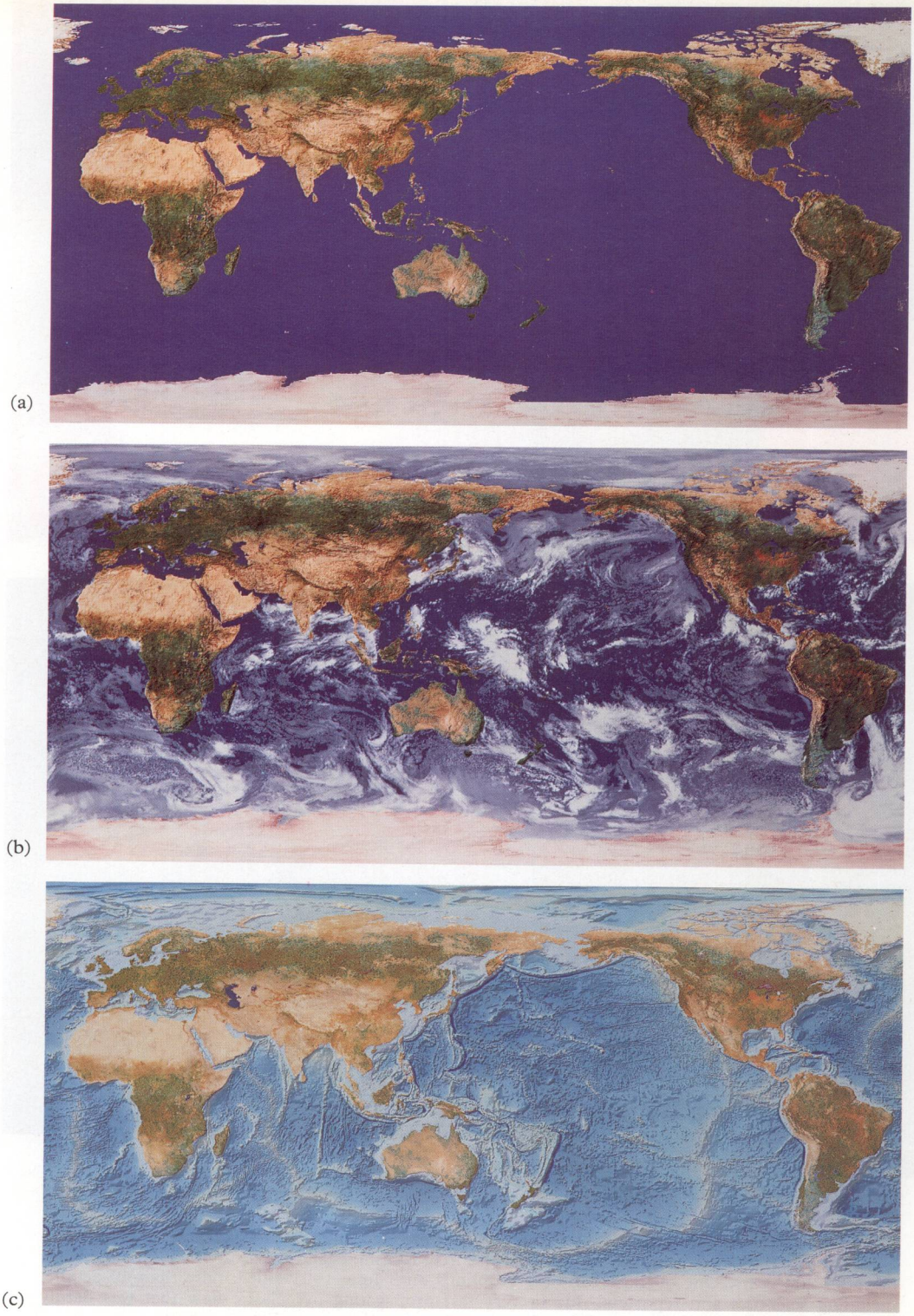

FIG. 10 (a), (b) AND (c). World map by computer mosaic from data of meteorological satellite (NOAA).

Image data of global land area and clouds were created by using NOAA GAC (global area coverage) data and observation data of geostational meteorological satellites, respectively. In order to create global cloud cover image, observation data of GMS (Japanese satellite), GOES (that of USA), METEOSAT (that of Europe), INSAT (that of India), and METE (that of USSR) were collected through communication lines and then were mosaiced: (a) global land image; (b) global land image and cloud cover; (c) composite image of global land and ocean.